Project Number: [956004]
Project Acronym: [BioTrib]
Project title: [**Advanced Research Training for the Biotribology of Natural and Artificial Joints in the 21st Century**]

Multi-scale modelling of flow through hierarchical porous cellular structures

Deliverable D4.1

Month Due: PM36

Month Delivered: PM36

Project coordinator name	Prof. Richard M Hall
Project coordinator organisation name	UNIVLEEDS
Report prepared by	Mahdieh Mosayebi Prof. Stephen Ferguson ETH Zürich

Dissemination Level of Report

PU	Public	
PP	Restricted to other program participants (including the Commission Services)	
RE	Restricted to a group specified by the consortium (including the Commission Services)	
CO	Confidential, only for members of the consortium (including the Commission Services)	X

The BioTrib ETN project has received funding from the European Union's Horizon 2020 research and innovation programme under grant agreement No. 956004.

Contents

Executive Summary

Osteoarthritis (OA), a prevalent joint disorder that affects an estimated 500 million adults worldwide, occurs when the protective cartilage that cushions the ends of bones wears down over time [1]. This degeneration leads to pain, stiffness, and reduced joint flexibility. Several factors contribute to the onset of osteoarthritis, including the natural aging process, genetics, traumatic injuries, and intense physical activities such as sports. As joints lose their ability to function correctly, individuals experience a decline in overall mobility and an increase in discomfort, often accompanied by severe pain. While medications, physical therapy, exercise, and various lifestyle adjustments are commonly employed as initial treatments for joint diseases, joint replacements stand out as a crucial and often ultimate solution. Partial or total joint replacements, like hip and knee replacements, involve replacing damaged joint surfaces with prosthetic implants, alleviating pain, and restoring joint functionality. However, the durability of these implants becomes a concern, especially in younger and more active patients who may outlive the typical lifespan of joint replacements, which currently ranges from 15 to 20 years, limited by failure due to wear and debris. Thus, studying the biotribology of joints is significant for optimizing the design of joint replacements, improving their performance, and ensuring longevity.

Biotribology, a multidisciplinary field, encompasses the study of friction, wear, and lubrication in biological systems. In the context of joint replacements, the significance of biotribology becomes evident as it elucidates the intricate dynamics of natural joint lubrication. The self-lubricating capabilities of natural articulating joints under load, attributed to the intrinsic poroelasticity of cartilage tissue and the self-pressurization of interstitial fluid, inspire enhancement of the design of prosthetic joints. Despite the pivotal role of lubrication in minimizing friction and wear, current studies have yet to produce a prosthesis capable of self-lubrication. This has prompted our pursuit of designing and developing a novel self-lubricating prosthesis, aiming to replicate the sophisticated natural lubrication regime observed in human joints. Accordingly, the objectives of this project will be accomplished through the following steps:

1. Development of a multiphysics model of the lubrication of the prosthesis
2. Deployment of a multiscale model of the self-lubricating prosthesis
3. Experimental validation

This report presents the progress towards aims 1 and 2, demonstrating through multi-scale simulation models the potential of flow-modifiying structures at the micrometre and millimetre scale to provide a non-uniform response under loading and unloading conditions. This may allow the creation of a prosthesis with an enhanced ability to produce and retain a lubricating fluid film under load.

Introduction

Synovial joints

Synovial joints, including a viscous fluid surrounded by the synovial membrane as well as the articular cartilage that covers bone surfaces, can freely move and withstand physiological loads due to their remarkable lubrication properties. Today, many people suffer from various joint diseases caused by several factors such as aging, trauma, or intense sports activities. Not only can degenerative joint diseases substantially reduce the patient's quality of life by leading to pain, disability, and social isolation, but also substantially enhance the socioeconomic costs of the disease. Total or partial replacements of the unhealthy joint with a prosthesis have currently been adopted as a solution to enhance stability, load capacity, and mobility, and to provide minimal friction and wear. It is predicted that the demand for the surgeries of total knee or hip replacements is set to rise considerably worldwide [2, 3]. The increasing number of younger people undergoing such orthopedic surgeries places additional demands on the performance and lifespan of prostheses. Therefore, much effort has been made to design longer-lasting and higher-performing prostheses to contribute to enhancing joint function, preventing revision surgeries, improving the quality of life of patients, and reducing the socioeconomic burden of such

diseases. Studies indicated the major issues that have a considerable influence on the failure of prostheses are wear and debris [4-6]. Wear debris can gradually be accumulated within the joint and lead to adverse biological responses and loosening of the prosthesis. Thus, investigation of the lubrication mechanisms that can minimize wear and debris is vital to extend the life of joint prostheses.

Lubrication

Biotribology, the study of friction, lubrication, and wear in biological systems, was first defined by Professor Duncan Dowson in the early 1970s [7, 8]. Indeed, understanding the lubrication of joint replacements can contribute to a full appreciation of the tribological behavior of such replacements. An empirical formula was developed to estimate the minimum film thickness in a full film lubrication regime in 1978 [9]. Hydrodynamic lubrication was first discovered by Tower while conducting a series of experiments between 1883 to 1891 [10, 11]. The results of the Tower's experiments inspired Osborne Reynolds to derive the Reynolds equation, governing hydrodynamic lubrication, from the Navier-Stokes equations in 1886 [12]. The Stribeck number, proposed by Stribeck in 1902, is a synthetic parameter combining load, velocity, as well as fluid viscosity, and is often used to differentiate between the lubrication regimes [13]. There are three primary lubrication regimes, namely full film lubrication, mixed lubrication, and boundary lubrication. Within the full film lubrication, the two surfaces are separated completely from each other by the fluid film leading to a lower friction coefficient. The mixed lubrication regime is a transient region between full film and boundary lubrication regimes. In the latter one, the surfaces are directly in contact resulting in a higher friction coefficient. The full film lubrication regime consists of two parts called elastohydrodynamic lubrication (EHL) and hydrodynamic lubrication (HL). The difference between these two parts is that the deformation of a solid structure needs to be addressed as well as the film thickness within the EHL regime, while the order of magnitude of the solid deformation is much smaller than the film thickness in the HL regime and can be neglected. It is noteworthy that the EHL regime has the lowest friction coefficient and is considered the optimal condition for lubrication.

The concept of weeping lubrication, or self-pressurized hydrostatic lubrication, has also been introduced by McCutchen as a possible mechanism in synovial joints due to the porous and deformable characteristics of cartilage [14-18]. McCutchen explained that the pressurized fluid in the porous cartilage discharges into the fluid domain between the contacting surfaces, forms, and maintains a lubricant film while subjected to the load [14]. According to this lubrication mechanism, this pressurized fluid mostly supports the applied load and a small fraction is supported by the solid structure of the articular cartilage, leading to minimizing friction. Later, McCutchen conducted a series of experiments indicating the animal joints are weeping bearings [16]. However, Walker et al. also introduced a new mode of lubrication called "boosted lubrication" to describe the load-bearing capability of synovial joints [19]. In the boosted lubrication, contrary to the weeping hypothesis, it was assumed that the water solvent and small molecular weight solutes of the synovial fluid would flow into the cartilage under loading and the remaining hyaluronic acid gel would act as a lubricant of the bearing surfaces. Then, Macirowski et al. confirmed the weeping lubrication mechanism of the human hip joint, proposed by McCutchen, numerically and experimentally, and mentioned that the inward flow into the porous cartilage only would be possible during the unloading phases [20]. This weeping lubrication mechanism could be considered as an alternative to the hydrodynamic or elastohydrodynamic lubrication regimes since it justifies the temporal response of the cartilage friction coefficient [21]. The following studies mostly focused on exploring the correlation between the interstitial fluid pressurization and the frictional response of the cartilage, irrespective of the fluid flow direction [22].

The early studies of lubrication were highly simplified due to the absence of any advanced computing power. These studies mostly focused on the line contact problems with contacts of infinite width and derived the deformation of the surfaces based on the Hertzian theory, which is for dry contacts, rather than considering the fluid pressure [23, 24]. Petrusevich solved the lubrication of a line contact problem which satisfied the Reynolds equation and derived deformation according to the fluid pressure [25]. Petrusevich's results gave the first great

insight into the behavior of EHL Lubrication. Dowson and Higginson later developed a series of numerical solutions to the EHL problem to determine the line contact EHL minimum film thickness [26-28]. Approximately 25 years later, Ranger et al. proposed the first numerical solution and indicated the typical point contact EHL characteristics [29]. It is worthwhile to mention that more powerful digital computers were required for point contact EHL problems and researchers could not have access to these resources widely.

Generally, it has been found that there is a lack of comprehensive understanding of the mechanisms underpinning lubrication [30, 31]. Suitable numerical modeling of joint implants can contribute to deepening knowledge as well as accelerating the design and performance prediction of a more reliable joint replacement. Many computational models based on Finite Element Method (FEM) have been developed to analyze contact stresses and stability of the joint replacements under complex loadings [32-34]. Many of these studies have neglected or simplified lubrication despite its great importance and impact on wear performance. This is primarily due to the complex geometry, multiple contacts, multiphysics modeling, and multiscale characteristics of the structure. Generally, EHL models solve the coupled fluid dynamics of lubricant and the elastic deformation of contacting bodies. In the past few years, considerable progress has been achieved in the simulation of synovial joints [35, 36]. There are more numerical studies of lubrication of the total hip replacements compared to that of the knee replacements [37-39]. Pascau et al. assessed the impact of prosthetic joint conformity on lubrication assuming two rigid bearing surfaces and merely hydrodynamic lubrication [40]. Mongkolwongrojin et al. simulated the transient behavior of the EHL film in an artificial knee joint under point contact conditions [41]. The results indicated that EHL fluid film thickness became larger as the contact area rose while the fluid film pressure declined. Su et al. performed a time-dependent EHL lubrication simulation for total knee replacements using the multigrid method and constrained column model [42]. Although this study assumed the lubricant to be a Newtonian fluid, it could provide insight into the prediction of the potential surface damage of knee prostheses. Later, Gao et Al. proposed a numerical study of transient non-Newtonian EHL lubrication of a hip prosthesis while considering the shear-thinning property of the synovial fluid [43]. In these studies, geometry simplifications were done and none of them was experimentally validated. It is noteworthy to mention that the concept of a self-lubricating joint prosthesis was initially proposed by Tepic in 1980 and 1993 [44, 45]. This invention provided dynamic lubrication, specifically for total hip prostheses, by designing a pumping system within the acetabular cup or femoral head to mimic the natural weeping lubrication of the cartilage. However, manufacturing these innovative ideas posed significant challenges due to the technological and mechanical limitations of that time.

Synovial fluid

One of the most significant factors in lubrication modeling is the lubricant viscosity. A variety of lubricants have been utilized, including deionized water, saline solutions, synovial fluid components (hyaluronic acid, lubricin, and phospholipids), diluted or undiluted bovine calf serum (BCS), bovine synovial fluid, and custom-made lubricants, to replace human joint synovial fluid. Cooke et al. measured the viscosity of the human synovial fluid at a low shear rate ($0.1–10^3$ s^{-1}) and reported an almost linear decrease in viscosity against shear rate [46]. Yao et al. investigated various fluids at a relatively higher shear rate (10^4 s^{-1}) and suggested that all the synovial fluids showed typical non-Newtonian shear thinning characteristics due to the presence of hyaluronic acid, while deionized water and both undiluted and di-luted BCS were Newtonian [47]. Later, Scholes and Unsworth highlighted the importance of the effect of the synovial fluid on the friction and lubrication of artificial joints by conducting friction tests with several different lubricants under various loading conditions [48]. Bortel et al. developed a synthetic synovial fluid which could better mimic the genuine synovial fluid and therefore, better simulate the in vivo lubrication of joint prostheses in 2015 [49]. Gao et al. conducted a numerical study to investigate the shear-thinning effect of the synovial fluid on the lubricating film of the hip replacement [43]. The consequences exhibited that the shear-thinning property of the synovial fluid has a considerable impact on both the magnitude and location of the minimum film thickness.

Measurement of film thickness

To experimentally observe the fluid film thickness, two different approaches have been employed, namely electrical resistivity and optical interferometry [4, 39, 50-53]. The latter approach is more accurate, measuring the central film thickness in the range of 1–1000 nm with a resolution of ± 1 nm. However, the optical interferometry technique can be utilized only in applications with simplified contacts and materials, or simple loadings and motions [39, 52]. To date, direct measurements of the lubricant film of joint replacements in the human body are still impossible due to the absence of appropriate monitoring techniques [4]. Moreover, it is still challenging to measure the lubrication film thickness of the joint replacements in vitro due to the complexity of their geometry, the combination of materials, and the physiological motions and loads experienced on a daily basis [4].

Overall, the main aim of the present research is to advance the performance of joint replacements through technical innovation and a deeper understanding of joint function. It is primarily focused on lubrication, one of the main aspects of biotribology, to mimic the natural lubrication regime of human joints. To the best of the our knowledge, the present study is the first which aims to design and develop a novel and manufacturable, self-lubricating prosthesis. The direct benefit of this would be to lengthen the lifespan of artificial joints and reduce the need for revision surgery, particularly for young and active patients.

Deliverable Description

According to the literature review, existing knee or hip replacements cannot emulate key tribological characteristics of natural cartilage, and this could be a reason for their less than optimal performance in situ. Inspired by the fact that all of the natural articulating joints are self-lubricating, we aim to design and develop a novel self-lubricating prosthesis to be able to substantially approach the natural performance of the joints and prolong the survival of the orthopaedic prostheses. To this end, structural and flow simulation methods are employed using COMSOL Multiphysics. A hierarchical multiscale numerical modeling approach is developed to assess the time-dependent, nonlinear, and fluid-structure interactive behavior of the prosthesis's components. The influence of non-Newtonian characteristics of the synovial fluid, reflecting shear thinning, over a typical gait loading cycle is then explored.

Deliverable Report

1. Materials and Methods

To mimic the natural lubrication regime of human joints, including self-pressurization of the lubricant under load in a synthetic prosthesis, a fluid-structure interactions (FSI) model is employed to couple both fluid dynamics and solid deformation utilizing COMSOL Multiphysics 6.1. At this stage, specific mechanical features, modeled as generic functional unit cells, are developed which would provide a direction-dependent, non-linear flow characteristic, as a first step towards a self-lubricating bearing surface with high fluid retention time. Here, structural heterogeneity and non-linear flow characteristics of the unit cells can together provide a means to design and control the net direction and rate of fluid exudation from a mechanical self-pressurizing prosthesis.

The second step is to combine these unit cell concepts into a joint-scale system to explore the fluid film development, dispersion, and depletion over a typical loading cycle. The hierarchical multiscale numerical modeling approach is developed for the first time to couple the interactions of the lubrication and deformation mechanisms in micro and macro scale systems of a hip prosthesis to assess the time-dependent, nonlinear, and fluid-structure interactive behavior of the prosthesis's components. The impact of lower scale response on the higher scale function, or evaluating the lubricant reservoir mechanics in relation to body-level loading is assessed

through multiscale modeling. Studying the interdependence between spatial scales could provide a comprehensive understanding of lubrication evolution through the intra-articular gap under a realistic physiological loading mode.

1.1 Boundary Conditions (BCs)

Laminar flow is utilized for the unit cell models, each simulating a channel with fixed obstacles, including V-shaped obstructions as well as "Tesla valves". A multiphysics model with fluid-structure interactions is employed for the joint-scale simulation in this study. In the FSI model, laminar flow is considered for fluid flow and a linear elastic material model is used for the solid mechanics. For the unit cell simulations, the outlet pressure is set to 0 MPa, and the inlet pressure is considered as a step pressure rising from 0 to 3 MPa and subsiding to 0 MPa after 1.1 seconds (Figure 1a). The transient loading is associated with the loading and unloading phases during walking. The gait loading data employed for the joint scale models in the present study, derived from the black curve in Figure 1b, represents the boundary load applied on the top of the acetabular cup in an axisymmetric model. This data, representing the average resultant force on the hip joint for ten subjects with an average body weight (BW) of 75 Kg, is obtained from the Orthoload database [54]. Additionally, the fluid domain is considered a deforming domain for a moving mesh. For the joint-scale simulations, the BCs are indicated in Figure 2, with the outlet pressure set to be 0 MPa, the lower part of the prosthesis fixed, and a boundary load applied to the top surface of the model.

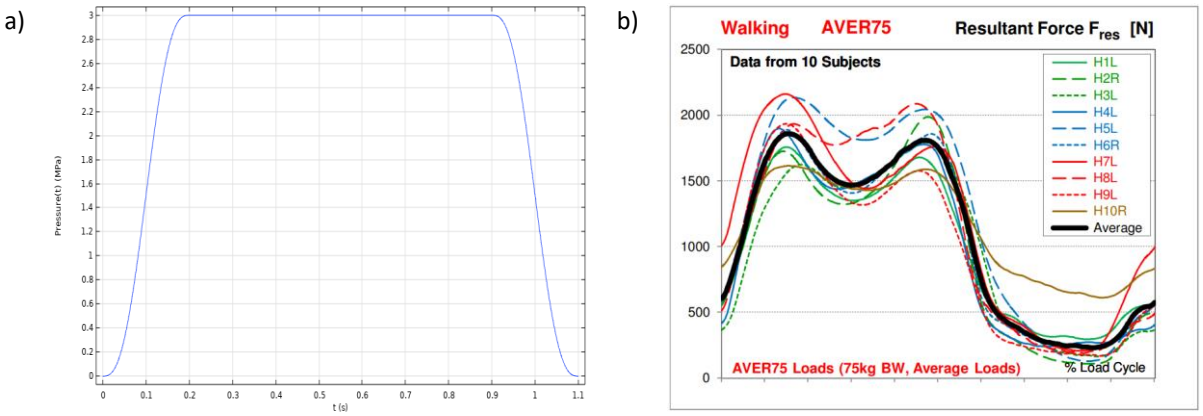

Figure 1 a: Applied physical pressure on unit cells during walking, b: resultant walking force data from 10 subjects based on Orthoload [52]

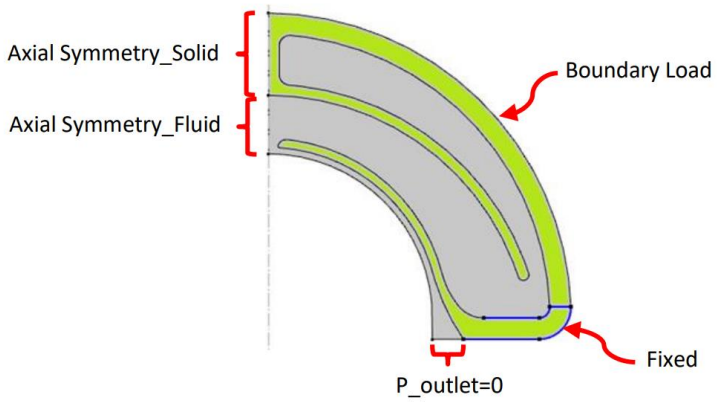

Figure 2 Boundary conditions for the joint-scale hip prosthesis in an axisymmetric FSI model, the green part represents the solid structure while the grey part indicates the fluid domain.

For simplicity, Newtonian fluid characteristics are initially considered for the synovial fluid with a density of 1225 kg/m^3 and dynamic viscosity of 1 Pa.s [55, 56]. As the shear-thinning property of the synovial fluid can substantially affect the lubrication film thickness distribution, non-Newtonian synovial fluid properties are considered in the asymmetric joint models, utilizing the Cross model [43]. The variation of viscosity (η) according to the shear rate ($\dot{\gamma}$) is expressed by Equation 1 [57].

$$\eta = \eta_\infty + \frac{\eta_0 - \eta_\infty}{1 + \alpha(\dot{\gamma})^\beta} \quad (1)$$

where, the limiting shear rate values for viscosity are η_0 = 40,000 mPas and η_∞ = 0.9 mPas. Analyzing synovial fluid viscosity values from eight different sources revealed that a suitable representation over a wide range of shear rates in joint replacements is achieved with α = 9.54 and β = 0.73 [43].

Two distinct materials, namely titanium alloy (Ti-6Al-4V Grade 5) and Ultra High Molecular Weight Polyethylene (UHMWPE), have been considered for the solid structure in the axisymmetric FSI model simulation. The mechanical properties of these bearing materials are listed in Table 1. The material properties for Ti-6Al-4V Grade 5 are derived by averaging the maximum and minimum values of the corresponding mechanical properties obtained from [58].

Table 1 Mechanical properties of the bearing materials [58, 59]

	Density (kg/m^3)	**Young's modulus (MPa)**	**Poisson's ratio**
Ti-6Al-4V	4470.5	114.5*10^3	0.34
UHMWPE	-	1016	0.46

2. Results and Discussion

2.1 Unit cells

A porous reservoir, situated between the acetabular cup and femoral head, was initially modeled. A multiphysics approach, or fluid-structure interaction model, was adopted to simulate a unit cell which is representative of one of the pores that would allow fluid flow to and from the bearing surface. A 2D transient symmetrical model was developed, featuring a functional unit cell with a small channel and two titanium leaflets, indicating the entrance of the Newtonian synovial fluid to the prosthesis. The direction dependency of the fluid flow through the channel was investigated for the rectangular leaflets with three different inclinations (Figure 3). The upper edge of the channel was considered as the symmetry line to reduce the computational costs. The ratios of the outlet velocity of the reverse flow to the outlet velocity of fluid flow in the normal upstream to downstream direction for the channel with leaflets with inclinations 0°, 15°, and 30° are 1, 0.36, and 0.44, respectively. Simulation results indicated therefore that the resistance to fluid flowing from upstream to downstream was different from that of fluid flowing in the opposite direction, with the exception obstruction leaflets with no inclination. Following this, a curved leaflet was chosen to help the fluid flow more smoothly. A sinus region was also added to the geometry, as such a region exists after all valves in human blood vessels (Figure 4). The shape of the leaflet indicated in Figure 4a was not suitable since the two leaflets met each other when the lubricant flowed from downstream to upstream. Then, a curved leaflet with a shorter length and smoother tip, presented in Figure 4b, was simulated which confirmed the direction dependency of the fluid flow through the channel.

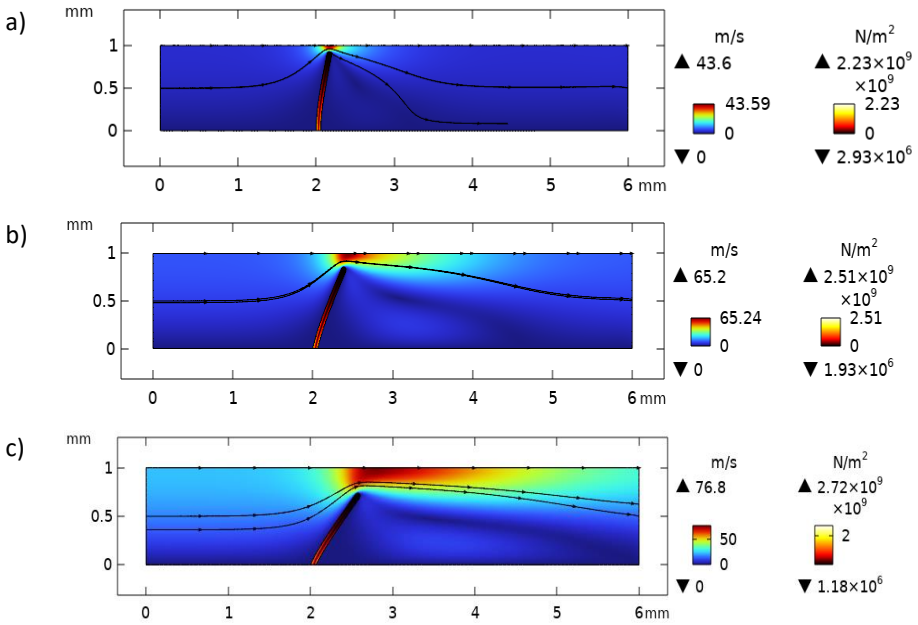

Figure 3 Velocity profile of the fluid and Von Mises stress of the leaflets in a 2D symmetrical model, with different inclinations of the leaflets

a) 0° b) 15° c) 30°

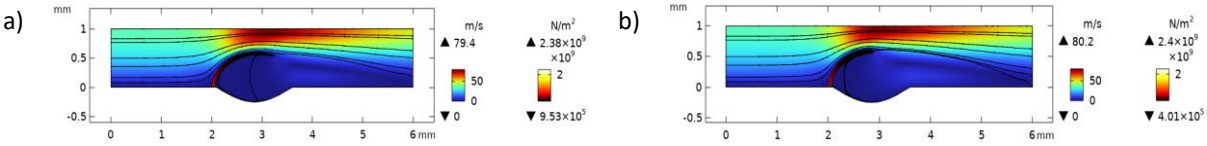

Figure 4 Velocity profile of the fluid and Von Mises stress of the curved leaflets in a symmetrical model a) longer leaflet with sharper tip b) shorter leaflet with smooth tip

Having established that this geometry could provide different resistances between flows in two different directions through the channel, 3D models were developed as exhibited in Figure 5. In the 3D multiphysics simulation, the fluid flow could not deflect the titanium leaflet, due to its high elastic modulus and self-reinforced geometry, and therefore the leaflet acted as a rigid wall (Figure 5a). The single structure of titanium leaflets was then split into four smaller leaflets to increase their flexibility, but the displacements of these leaflets were negligible as well (Figure 5b). The two last steps were performed once more by considering a shell rather than a solid structure to reduce the computational cost (Figures 5c and 5d).

To address this lack of desired performance, it was proposed to change the assumed unit cell geometry to “Tesla valves” to enhance the direction-dependent resistance of the fluid flow through the channel, employing laminar flow. The velocity fields of fluid flow from upstream to downstream and the reverse fluid flow through a Tesla valve in a steady state condition are shown in Figures 6a and 6b, respectively. Tracing fluid from upstream to downstream suggested that the fluid did not get trapped in the loops and went through the straight path, while the reverse flow met secondary flow coming back from the turns of the Tesla valve where the resulting vortices caused a higher resistance. This results in a 22.21% reduction of the average velocity of the outlet surfaces, from 35.12 m/s to 27.32 m/s. The effect of flow tortuosity through the Tesla valve was also confirmed for transient flow conditions, with different resistances observed in two different directions (13.62% reduction in outlet velocity at time 0.6 s). However, as Tesla valves are designed for high velocities, they do not demonstrate the same direction dependence for physiological synovial fluid velocities on the order of millimeters per second or lower. The negligible 0.7% difference in average outlet velocity between the flows in unit cell levels in Figures 6c and 6d confirms this.

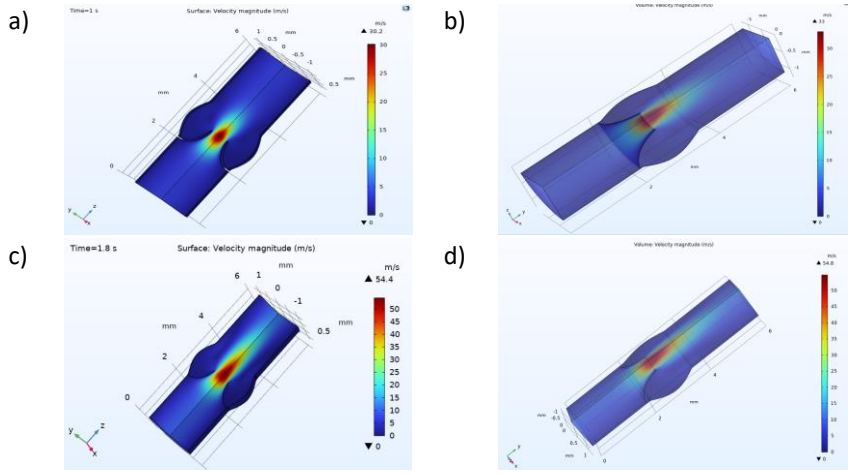

Figure 5 Velocity field of the fluid flow in a 3D channel with a) a single leaflet b) four-split leaflets c) a single shell, and d) four-split shell leaflets

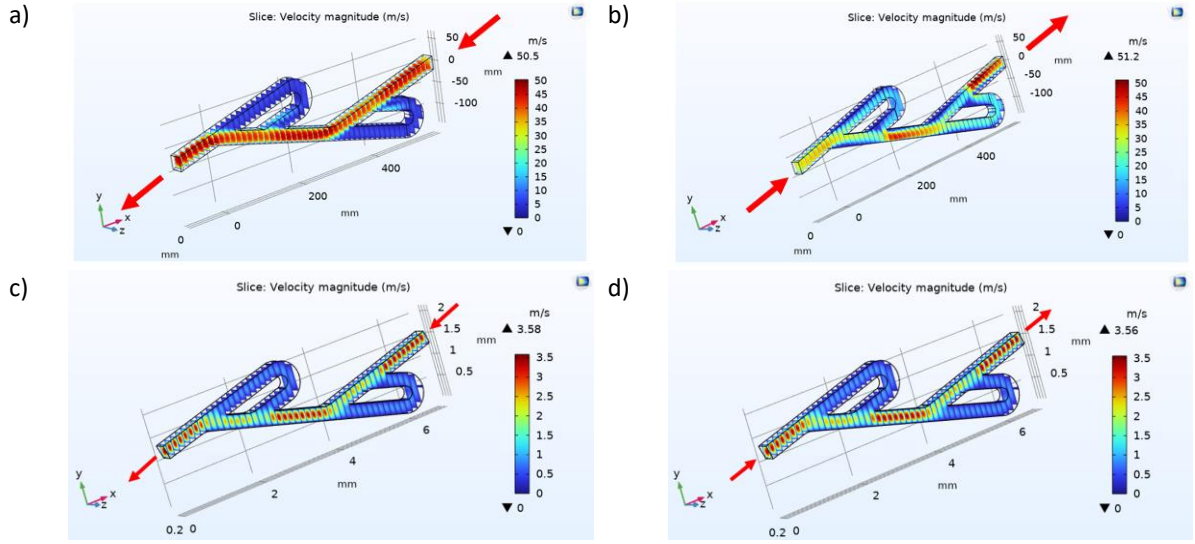

Figure 6 Velocity field of the fluid flow in Tesla valve in a steady state condition a) fluid flow from upstream to downstream in large scale model and b) reverse flow in large scale model c) fluid flow from upstream to downstream in a unit cell, and d) reverse flow in a unit cell. The red arrows show the direction of the inlet and outlet flows.

2.2 Joint-scale model

Although Tesla valves did not meet the functional requirements of the current study, they served as inspiration for a design that not only does not have moving structures but also can create nonlinear resistance to fluid flow through the channel. This can eliminate the high risk of fatigue, and therefore, extend the lifespan of the prosthesis. Figure 7 illustrates the velocity field of the examples of various designs of flow obstructions with fixed obstacles within the channel (10mm*32mm), creating different resistances to fluid flow in opposing directions at time 0.6 s. In this case, the lubricant would flow into the prosthesis under physiological loading and would flow back to the reservoir during the unloading phase, representing the dominant weeping lubrication in natural joints. In this section, the influence of the number, orientation, size, and diverse geometrical configurations of these obstacles as well as the length of the intermediate shell has been investigated. Creating small gaps between the barriers or the intermediate shell and the wall of the reservoir would locally increase the Reynolds number, contributing to the enhancement of flow nonlinearity. The highest and lowest ratios of

average outlet velocity to average inlet velocity are 19.09 and 2.22, corresponding to Figures 7f and 7h, respectively. One challenge with all these designs is the achievement of nonlinearities only at high velocities, as observed in Tesla valves, making them unsuitable for low velocities induced by joint loading. Additionally, fabricating these designs in 3D poses another issue, as having the fixed structures positioned independently without interconnection proves challenging. One potential solution involves connecting them using small lattice structures. However, this approach requires careful examination of its impact on fluid flow through the lubricant reservoir and consideration of potential endurance limitations, introducing further challenges.

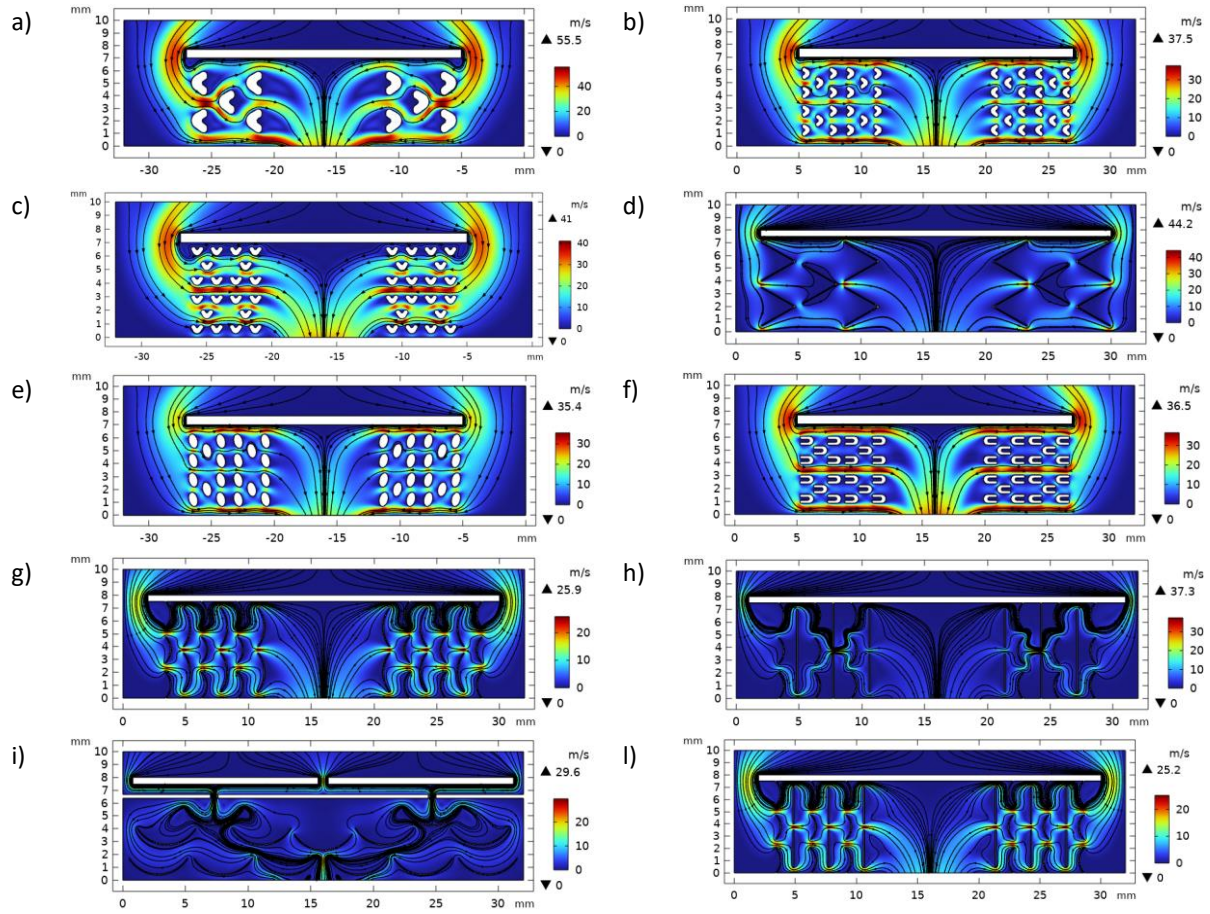

Figure 7 Velocity field of the examples of various designs of flow obstruction with different numbers, orientations, sizes, and diverse geometrical configurations for fixed obstacles within the channel at time 0.6 s. The black lines represent the velocity streamlines.

Following these investigations, the distributed obstacles were eliminated to advance toward designs that are easier to fabricate. Examples of such designs are exhibited in Figure 8. In these designs, the lubricant reservoir (10mm*32mm) as well as the lubrication film (0.6mm*32mm) are modeled. It is noteworthy that the thickness of the lubrication film is exaggerated in order to simplify the numerical problem and reduce the computational costs. The impact of the number of hemispherical obstacles, gap sizes between them, length of the intermediate shell, the addition of throats between the reservoir and the lubrication film, the incorporation of a porous layer as well as two additional intermediate shells, and the transition to a hemispherical shape of the reservoir is explored. The comparison of the effect of these changes on nonlinearity and asymmetry through the lubricant reservoir is shown in Figure 8g. To assess nonlinearity and asymmetry, Dirichlet Boundary Conditions are employed in a stationary study. An inlet velocity ranging from -50 mm/s to 50 mm/s with intervals of 10 mm/s is applied on the upper edge of the reservoir and the outlet pressure on the two ends of the lubrication film is set to 0 MPa. Subsequently, the pressure of the inlet part is investigated. At a consistent inlet velocity, the greater the inlet pressure, the higher the resistance becomes, signifying a more nonlinear geometry. In other words, the resistance to flow is reflected in the slope of the curves in Figure 8g. Asymmetry represents

differences in fluid flow behavior when squeezing out towards the lubrication film compared to the flow back to the reservoir.

The results highlighted that adding throats and a longer intermediate shell each enhances the nonlinearity within the channel while decreasing asymmetry. The incorporation of a porous layer significantly increases resistance while simultaneously decreasing asymmetry considerably. In contrast, increasing the number of obstacles with the same gap size between them leads to a decline in resistance and an enhancement in asymmetry. Decreasing the distances between the hemispherical obstacles enhances the resistance and has an adverse effect on asymmetry. Furthermore, considering a distribution of distances between the hemispherical obstacles, as depicted in Figure 8d, results in diminishing the resistance and an enhancement in asymmetry. The addition of two more intermediated shells, as illustrated in Figure 8e, significantly increases asymmetry as well as the difference between the resistances in two opposite directions. Figure 8g explicitly suggests that the hemispherical prosthesis induces a dramatic change in resistances to flow in two different directions and asymmetry. It is worthwhile to mention that one of the novelties of the present study is that the designed geometries, as depicted in Figure 8, can provide distinct resistances between flows in two different directions through the channel even though the magnitudes of the velocities are small and are in the order of millimeters per second, fulfilling an expectation that Tesla valves could not meet. From the biotribological perspective, the designed non-linear geometries induce different resistances for synovial fluid flowing into and out of the intra-articular gap, enhancing the retention time of a self-pressurized load-bearing fluid component in the joint.

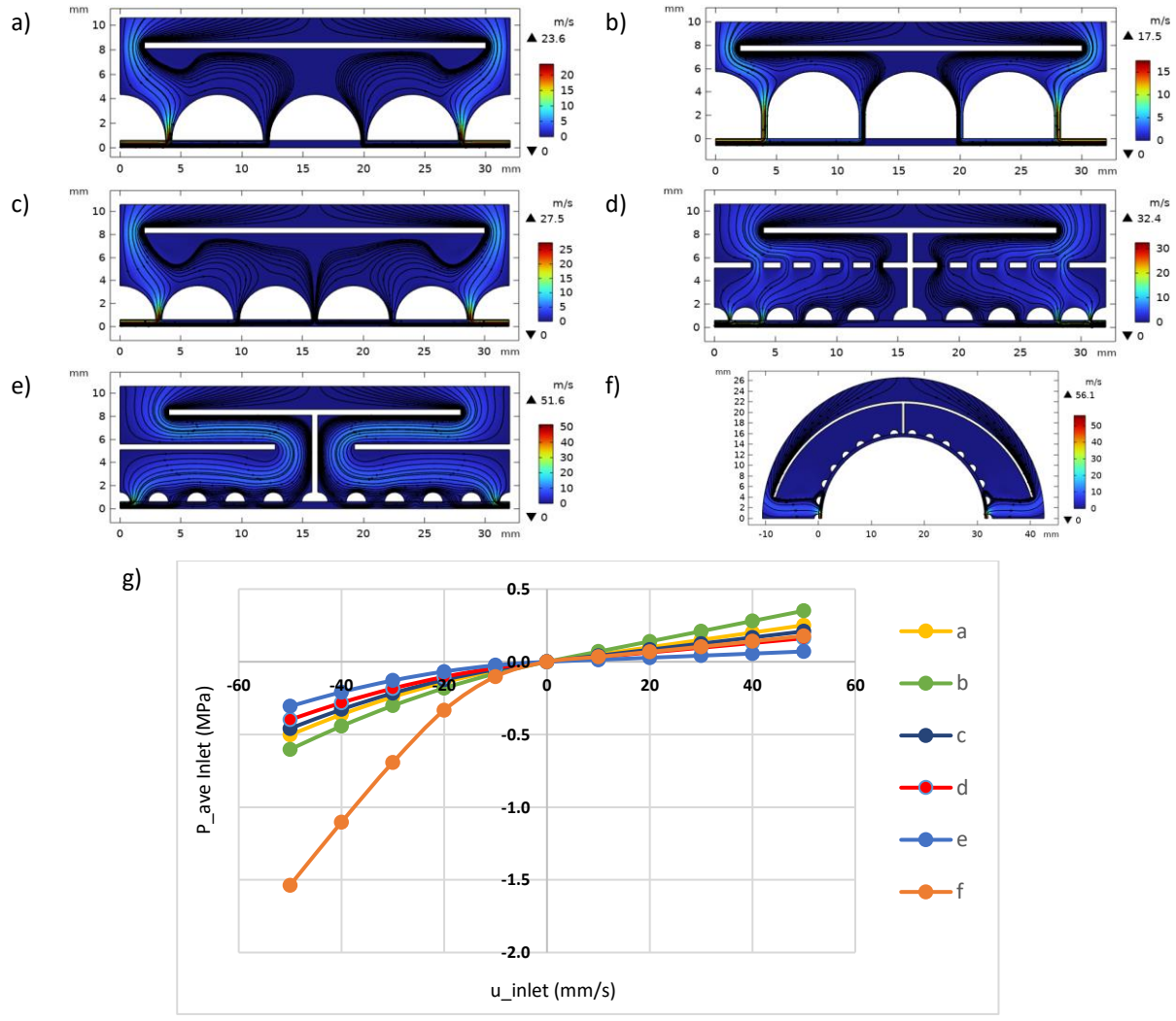

Figure 8 Velocity field of the examples of various designs of flow obstruction with different numbers of hemispherical obstacles, gap sizes between them, length of the intermediate shell, the addition of throats between the reservoir and the lubrication film (b), the incorporation

of a porous layer (d) as well as two additional intermediate shells (e), and the transition to a hemispherical shape of the reservoir (f) at time 0.6 s. g) the comparison of the effect of these changes on nonlinearity and asymmetry through the lubricant reservoir. The black lines represent the velocity streamlines.

Having established that the developed 2D joint-scale model of a self-lubricating hip prosthesis based on realistic joint geometry, Figure 8f, offered different resistances between flows in two opposite directions through the channel, 3D models are developed as exhibited in Figure 9. As demonstrated in Figure 9, the reservoir exclusively supplies the lubrication film through the last two layers of the porous outer layer under loading, and therefore, a negligible amount of fluid would exude in the upper part of the prosthesis. To address this issue, a continuous outer layer would be considered to let the fluid squeeze out through a central orifice (Figure 10). In the next step, the model has been improved to a 2D axisymmetric model to reduce the computational cost. Furthermore, non-Newtonian characteristics of the synovial fluid based on the Cross model have been taken into consideration. Figure 10 demonstrates the velocity field of fluid flow, displacement of the solid structure, and viscosity variation of the synovial fluid through a joint scale self-lubricating hip prosthesis in an axisymmetric simulation with consideration of two distinct materials, namely UHMWPE and Ti-6Al-4V, at 0.4 (loading phase) and 0.9 s (unloading phase) during a gait loading cycle.

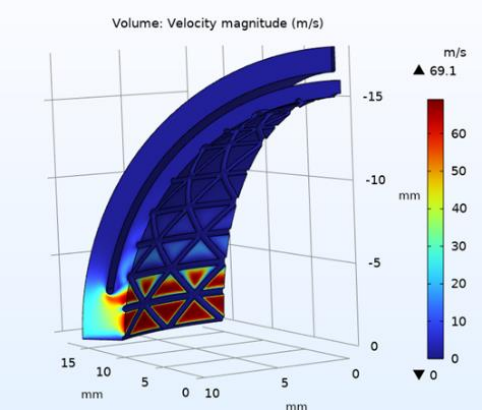

Figure 9 Velocity field through a 3D element of the lubricant reservoir with symmetry boundary conditions on the lateral sides under loading phase

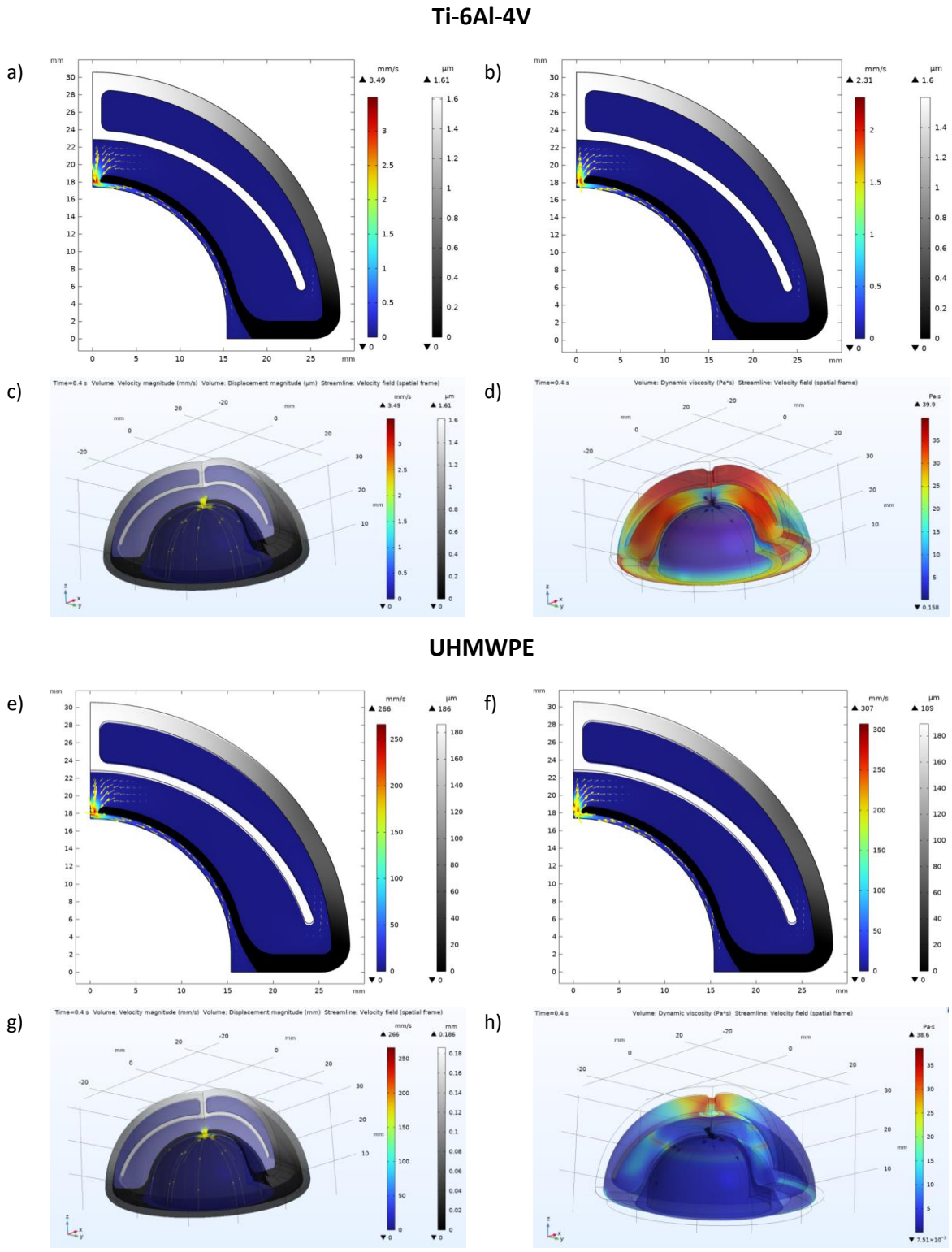

Figure 10 A joint scale self-lubricating hip prosthesis in an axisymmetric simulation made of Ti-6Al-4V: a) velocity and displacement fields under loading at 0.4s, b) velocity and displacement fields under unloading at 0.9 s, c) velocity field within a revolution angle 240 degrees at 0.4s, d) viscosity variation within a revolution angle 240 degrees at 0.4s, and made of UHMWPE: e) velocity and displacement fields under loading at 0.4s, f) velocity and displacement fields under unloading at 0.9 s, g) velocity field within a revolution angle 240 degrees at 0.4s, and h) viscosity variation within a revolution angle 240 degrees at 0.4s. The yellow and black lines represent the velocity streamlines.

Results confirm that during the loading phase, such as at 0.4 s, fluid within the pumping membrane of the hip prosthesis squeezes out, and subsequently flows back to the reservoir during the unloading phase, for instance, at 0.9 s. This observed behavior is consistent for both Ti-6Al-4V and UHMWPE prostheses and is depicted by the yellow streamlines in Figures 10a, 10b, 10e, and 10f. A 2D axisymmetric simulation can also provide a three-dimensional view of the results. Figure 10d suggests that synovial fluid within the Ti-6Al-4V prosthesis has high viscosity in most parts at 0.4s, whereas Figure 10h indicates that synovial fluid with low viscosity dominates the UHMWPE prosthesis. This discrepancy arises from the higher flexibility of UHMWPE compared to Ti-6Al-4V. Figures 10a and 10e demonstrate that the displacement of UHMWPE (186 µm) is substantially higher than that of the Ti-6Al-4V prosthesis (1.61 µm) at 0.4 s. Consequently, the shear rate is higher for the UHMWPE prosthesis, leading to lower viscosity of the synovial fluid and facilitating easier flow under physiological loading modes, as predicted by the Cross model. This phenomenon explains the reason for the lower velocity and therefore a diminished flow rate through the Ti-6Al-4V prosthesis compared to the UHMWPE one (Figures 10c, 10g, and 11).

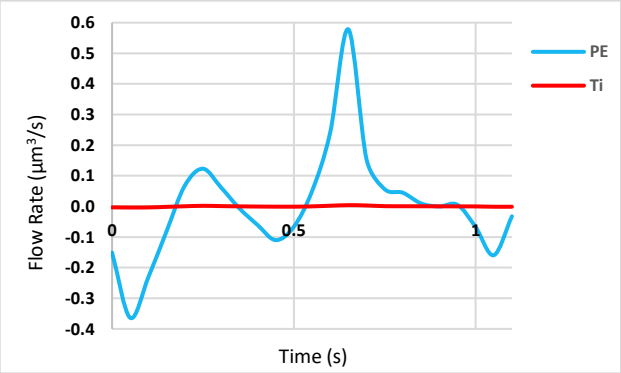

Figure 11 Flow rate through the outlet part of the joint scale self-lubricating hip prosthesis with different materials, namely UHMWPE and Ti-6Al-4V, over a gait loading cycle

Summary

Existing knee or hip replacements cannot emulate key tribological characteristics of natural cartilage, and this could be a reason for their less than optimal performance in situ. Inspired by the fact that all of the natural articulating joints are self-lubricating, we aim to design and develop a novel self-lubricating prosthesis. This involves a variety of computational models that will advance the standard of joint lubrication modeling, considering for example multi-scale flow phenomena and multiphysics modeling. As a first step towards a self-lubricating bearing surface with high fluid retention time, specific mechanical features, modeled as functional unit cells, are developed which provide a direction-dependent, non-linear flow characteristic. Subsequently, various non-linear geometries were designed to induce different resistances for the synovial fluid flowing into and out of the intra-articular gap, leading to enhancement of the retention time of a self-pressurized load-bearing fluid component in the joint. Then, synovial fluid flow within a joint scale Ti-6Al-4V and UHMWPE prostheses, fluid film development, and displacement of the solid structures over a typical gait loading cycle are explored, demonstrating a potential load-induced self-lubrication. Moreover, the non-Newtonian characteristics of the synovial fluid have been taken into account despite their complexity in numerical problems.

For the next step of this study, some microstructures developed earlier may be incorporated into the current hip prosthesis geometry to enhance the nonlinearity aspects. Following that, the material selection will be finalized, taking into account the advanced additive manufacturing criteria and limitations. This will pave the way for the final step of the project, which involves fabricating the prototype systems and validating the numerical results experimentally.

Overall, this study primarily focused on lubrication, one of the main aspects of biotribology, to mimic the natural lubrication regime of human joints and consequently contribute to lengthening the lifespan of artificial joints. The definite benefit of this would be reducing the need for revision surgery, particularly for young and active patients, and greatly contributing to enhancing the quality of life of patients.

References

[1] Q. Yao *et al.*, "Osteoarthritis: pathogenic signaling pathways and therapeutic targets," *Signal Transduction and Targeted Therapy,* vol. 8, no. 1, p. 56, 2023.

[2] A. Ford, Z. Hua, S. J. Ferguson, L. A. Pruitt, and L. Gao, "A 3D-transient elastohydrodynamic lubrication hip implant model to compare ultra high molecular weight polyethylene with more compliant polycarbonate polyurethane acetabular cups," *Journal of the Mechanical Behavior of Biomedical Materials,* vol. 119, p. 104472, 2021.

[3] L. Wang, G. Isaac, R. Wilcox, A. Jones, and J. Thompson, "Finite element analysis of polyethylene wear in total hip replacement: A literature review," *Proceedings of the Institution of Mechanical Engineers, Part H: Journal of Engineering in Medicine,* vol. 233, no. 11, pp. 1067-1088, 2019.

[4] L. Gao, X. Lu, X. Zhang, Q. Meng, and Z. Jin, "Lubrication Modelling of Artificial Joint Replacements: Current Status and Future Challenges," *Lubricants,* vol. 10, no. 10, p. 238, 2022.

[5] L. Mattei, F. Di Puccio, B. Piccigallo, and E. Ciulli, "Lubrication and wear modelling of artificial hip joints: A review," *Tribology International,* vol. 44, no. 5, pp. 532-549, 2011.

[6] Y. Su, P. Yang, Z. Fu, Z. Jin, and C. Wang, "Time-dependent elastohydrodynamic lubrication analysis of total knee replacement under walking conditions," *Computer Methods in Biomechanics and Biomedical Engineering,* vol. 14, no. 06, pp. 539-548, 2011.

[7] D. Dowson, "Review paper 2: whither tribology?," in *Proceedings of the Institution of Mechanical Engineers, Conference Proceedings*, 1969, vol. 184, no. 12: SAGE Publications Sage UK: London, England, pp. 181-185.

[8] D. Dowson, "Bio-tribology," *The Rheology of Lubricants,* vol. 81, 1973.

[9] B. J. Hamrock and D. Dowson, "Elastohydrodynamic lubrication of elliptical contacts for materials of low elastic modulus I—fully flooded conjunction," 1978.

[10] B. Tower, "First report on friction experiments," *Proceedings of the institution of mechanical engineers,* vol. 34, no. 1, pp. 632-659, 1883.

[11] F. Archibald, "History of lubrication," *Tribology & Lubrication Technology,* vol. 55, no. 9, p. 9, 1999.

[12] O. Reynolds, "IV. On the theory of lubrication and its application to Mr. Beauchamp tower's experiments, including an experimental determination of the viscosity of olive oil," *Philosophical transactions of the Royal Society of London,* no. 177, pp. 157-234, 1886.

[13] R. Stribeck, "Die wesentlichen eigenschaften der gleit-und rollenlager," *Zeitschrift des Vereines Deutscher Ingenieure,* vol. 46, pp. 1341-1348, 1432-1438, 1463-1470, 1902.

[14] C. McCutchen, "Mechanism of animal joints: sponge-hydrostatic and weeping bearings," *Nature,* vol. 184, no. 4695, pp. 1284-1285, 1959.

[15] P. Lewis and C. McCutchen, "Mechanism of animal joints: experimental evidence for weeping lubrication in mammalian joints," *Nature,* vol. 184, no. 4695, pp. 1285-1285, 1959.

[16] C. W. McCutchen, "The frictional properties of animal joints," *Wear,* vol. 5, no. 1, pp. 1-17, 1962.

[17] C. W. McCutchen, "Paper 1: physiological lubrication," in *Proceedings of the Institution of Mechanical Engineers, Conference Proceedings*, 1966, vol. 181, no. 10: SAGE Publications Sage UK: London, England, pp. 55-62.

[18] C. McCutchen, "Lubrication of and by articular cartilage," in *Cartilage*: Elsevier, 1983, pp. 87-107.

[19] P. Walker, D. Dowson, M. Longfield, and V. Wright, "" Boosted lubrication" in synovial joints by fluid entrapment and enrichment," *Annals of the Rheumatic Diseases,* vol. 27, no. 6, p. 512, 1968.

[20] T. Macirowski, S. Tepic, and R. W. Mann, "Cartilage stresses in the human hip joint," 1994.

[21] G. A. Ateshian, "The role of interstitial fluid pressurization in articular cartilage lubrication," *Journal of biomechanics,* vol. 42, no. 9, pp. 1163-1176, 2009.

[22] R. Krishnan, M. Kopacz, and G. A. Ateshian, "Experimental verification of the role of interstitial fluid pressurization in cartilage lubrication," *Journal of orthopaedic research,* vol. 22, no. 3, pp. 565-570, 2004.

[23] A. Ertel, "Hydrodynamic lubrication based on new principles," *Akad. Nauk SSSR Prikadnaya Mathematica i Mekhanika,* vol. 3, no. 2, pp. 41-52, 1939.

[24] A. Grubin, "Fundamentals of the hydrodynamic theory of lubrication of heavily loaded cylindrical surfaces," *Investigation of the Contact Machine Componets,* vol. 2, 1949.

[25] A. Petrusevich, "The basic conclusions from the elasto-hydrodynamic theory of lubrication," *Izv. Akad. Nauk SSSR, Odt. Tekhn. Nauk,* no. 2, p. 209, 1951.

[26] D. Dowson and G. Higginson, "A numerical solution to the elasto-hydrodynamic problem," *Journal of mechanical engineering science,* vol. 1, no. 1, pp. 6-15, 1959.

[27] D. Dowson and G. Higginson, "The effect of material properties on the lubrication of elastic rollers," *Journal of Mechanical Engineering Science,* vol. 2, no. 3, pp. 188-194, 1960.

[28] D. Dowson, "New roller-bearing lubrication formula," *Engineering Lond.,* vol. 192, p. 158, 1961.

[29] A. Ranger, C. Ettles, and A. Cameron, "The solution of the point contact elasto-hydrodynamic problem," *Proceedings of the Royal Society of London. A. Mathematical and Physical Sciences,* vol. 346, no. 1645, pp. 227-244, 1975.

[30] D. Nečas *et al.*, "Observation of lubrication mechanisms in knee replacement: a pilot study," *Biotribology,* vol. 17, pp. 1-7, 2019.

[31] D. Nečas *et al.*, "The effect of albumin and γ-globulin on synovial fluid lubrication: Implication for knee joint replacements," *Journal of the mechanical behavior of biomedical materials,* vol. 113, p. 104117, 2021.

[32] B. J. Fregly, W. G. Sawyer, M. K. Harman, and S. A. Banks, "Computational wear prediction of a total knee replacement from in vivo kinematics," *Journal of biomechanics,* vol. 38, no. 2, pp. 305-314, 2005.

[33] S. T. O'Brien, Y. Luo, and J.-M. Brandt, "In-vitro and in-silico investigations on the influence of contact pressure on cross-linked polyethylene wear in total knee replacements," *Wear,* vol. 332, pp. 687-693, 2015.

[34] Z. Jin, J. Zheng, W. Li, and Z. Zhou, "Tribology of medical devices," *Biosurface and Biotribology,* vol. 2, no. 4, pp. 173-192, 2016.

[35] S. Affatato and A. Ruggiero, "A perspective on biotribology in arthroplasty: From in vitro toward the accurate In Silico wear prediction," *Applied Sciences,* vol. 10, no. 18, p. 6312, 2020.

[36] A. Ruggiero, "Milestones in natural lubrication of synovial joints," *Frontiers in Mechanical Engineering,* vol. 6, p. 52, 2020.

[37] A. Ruggiero, A. Sicilia, and S. Affatato, "In silico total hip replacement wear testing in the framework of ISO 14242-3 accounting for mixed elasto-hydrodynamic lubrication effects," *Wear,* vol. 460, p. 203420, 2020.

[38] A. Ruggiero and A. Sicilia, "Lubrication modeling and wear calculation in artificial hip joint during the gait," *Tribology International,* vol. 142, p. 105993, 2020.

[39] X. Lu *et al.*, "Towards the direct validation of computational lubrication modelling of hip replacements," *Tribology International,* vol. 146, p. 106240, 2020.

[40] A. Pascau, B. Guardia, J. A. Puertolas, and E. Gómez-Barrena, "Knee model of hydrodynamic lubrication during the gait cycle and the influence of prosthetic joint conformity," *Journal of Orthopaedic Science,* vol. 14, no. 1, pp. 68-75, 2009.

[41] M. Mongkolwongrojn, K. Wongseedakaew, and F. E. Kennedy, "Transient elastohydrodynamic lubrication in artificial knee joint with non-Newtonian fluids," *Tribology International,* vol. 43, no. 5-6, pp. 1017-1026, 2010.

[42] Y. SU, Z. FU, P. YANG, and C. WANG, "A full numerical analysis of elastohydrodynamic lubrication in knee prosthesis under walking condition," *Journal of Mechanics in Medicine and Biology,* vol. 10, no. 04, pp. 621-641, 2010.

[43] L. Gao, D. Dowson, and R. W. Hewson, "A numerical study of non-Newtonian transient elastohydrodynamic lubrication of metal-on-metal hip prostheses," *Tribology International,* vol. 93, pp. 486-494, 2016.

[44] S. Tepic, "Compliant head femoral endoprostheses," Patent 4,318,191, 1980.

[45] S. Tepic, "Lubricated cup for total joint prosthesis," Patent EP0 663 810 B1, 1993.

[46] A. Cooke, D. Dowson, and V. Wright, "The rheology of synovial fluid and some potential synthetic lubricants for degenerate synovial joints," *Engineering in Medicine,* vol. 7, no. 2, pp. 66-72, 1978.

[47] J. Yao, M. Laurent, T. Johnson, C. Blanchard, and R. Crowninshield, "The influences of lubricant and material on polymer/CoCr sliding friction," *Wear,* vol. 255, no. 1-6, pp. 780-784, 2003.

[48] S. Scholes and A. Unsworth, "The effects of proteins on the friction and lubrication of artificial joints," *Proceedings of the Institution of Mechanical Engineers, Part H: Journal of Engineering in Medicine,* vol. 220, no. 6, pp. 687-693, 2006.

[49] E. L. Bortel, B. Charbonnier, and R. Heuberger, "Development of a synthetic synovial fluid for tribological testing," *Lubricants,* vol. 3, no. 4, pp. 664-686, 2015.

[50] N. Ohtsuki, T. Murakami, S. Moriyama, and H. Higaki, "Influence of geometry of conjunction on elastohydrodynamic film formation in knee prostheses with compliant layer," in *Tribology Series*, vol. 32: Elsevier, 1997, pp. 349-359.

[51] D. Dowson, C. McNie, and A. Goldsmith, "Direct experimental evidence of lubrication in a metal-on-metal total hip replacement tested in a joint simulator," *Proceedings of the Institution of Mechanical Engineers, Part C: Journal of Mechanical Engineering Science,* vol. 214, no. 1, pp. 75-86, 2000.

[52] D. Nečas, M. Vrbka, F. Urban, J. Gallo, I. Křupka, and M. Hartl, "In situ observation of lubricant film formation in THR considering real conformity: The effect of diameter, clearance and material," *Journal of the mechanical behavior of biomedical materials,* vol. 69, pp. 66-74, 2017.

[53] D. Nečas *et al.*, "Towards the understanding of lubrication mechanisms in total knee replacements–Part I: experimental investigations," *Tribology International,* vol. 156, p. 106874, 2021.

[54] [Online]. Available: https://orthoload.com/

[55] J. Schurz and V. Ribitsch, "Rheology of synovial fluid," *Biorheology,* vol. 24, no. 4, pp. 385-399, 1987.

[56] Y. Wu and S. J. Ferguson, "The influence of cartilage surface topography on fluid flow in the intra-articular gap," *Computer methods in biomechanics and biomedical engineering,* vol. 20, no. 3, pp. 250-259, 2017.

[57] M. M. Cross, "Rheology of non-Newtonian fluids: a new flow equation for pseudoplastic systems," *Journal of colloid science,* vol. 20, no. 5, pp. 417-437, 1965.

[58] [Online] Available: https://www.azom.com/properties.aspx?ArticleID=1547

[59] J. SHI, "Finite element analysis of total knee replacement considering gait cycle load and malalignment," degree of Doctor of Philosophy, University of Wolverhampton, 2007.